Phase and Morphology Changes in Lipid Monolayers Induced by SP-B Protein and Its Amino-Terminal Peptide

M. M. Lipp, K. Y. C. Lee, J. A. Zasadzinski,* A. J. Waring

Both human lung surfactant protein, SP-B, and its amino-terminal peptide, SP-B_{1-25}, inhibit the formation of condensed phases in monolayers of palmitic acid, resulting in a new fluid phase. This fluid phase forms a network, separating condensed-phase domains at coexistence. The network persists to high surface pressures, altering the nucleation, growth, and morphology of monolayer collapse structures, leading to lower surface tensions on compression and more reversible respreading on expansion. The network is stabilized by the low line tension between the fluid phase and the condensed phase as confirmed by the formation of "stripe" phases.

Human lung surfactant, a complex mixture of lipids and proteins, forms monolayers at the alveolar air-water interface that can lower the surface tension, γ, to near zero (*1*, *2*). A lack of surfactant, due to either immaturity in premature infants or disease or trauma in adults, can result in respiratory distress syndrome (RDS) (*2*, *3*). Administration of exogenous surfactant is an effective treatment for neonatal RDS, but supplies of human lung surfactant are limited and therefore replacement surfactants are derived primarily from animals (*4*). Concerns over potential viral contamination and immunological responses from animal-derived products, however, make developing synthetic lipids and synthetic or genetically engineered proteins tailored to specific RDS applications a major goal of research.

Developing a purely synthetic surfactant requires a thorough understanding of the roles of the individual lipid and protein constituents of natural surfactants, especially the amphiphilic protein SP-B and the anionic lipids that are necessary for surfactant function in vivo (*5*). Lung surfactant consists primarily of dipalmitoylphosphatidylcholine (DPPC), unsaturated phosphatidylcholines, unsaturated phosphatidylglycerols (PGs), palmitic acid (PA), and SP-B and SP-C (*2*, *6*). Pure DPPC can form monolayers that attain near zero values of γ (or high collapse pressures) on compression (*1*); however, DPPC adsorbs and respreads slowly as a monolayer under physiological conditions (*2*, *7*, *8*).

The unsaturated and anionic lipids present in natural surfactants and added to many replacement surfactants are believed to enhance the adsorption and respreading of DPPC (*7*, *8*). Palmitic acid is one of three compounds added to exogenous surfactant in Survanta (8.5% w/w; Ross Laboratories, Columbus, Ohio) and Surfactant TA (8.5% w/w; Tokyo Tanabe) used to treat premature infants with neonatal RDS. Because pure fatty acid and unsaturated PG monolayers have relatively low collapse pressures relative to DPPC, it has been hypothesized that lung surfactant monolayers are refined by selective removal of the lipids that have low collapse pressures on repeated compression and expansion, a phenomenon known as "squeeze-out" (*8*). However, the addition of whole SP-B or its NH_2-terminal peptide, SP-B_{1-25} (*9*–*12*), to monolayers of PA results in much higher monolayer collapse pressures (lower γ values) than those found in monolayers of either PA or SP-B alone. This result suggests a synergistic effect between PA and SP-B or SP-B_{1-25} that results in the retention of both lipid and protein in the primarily DPPC surfactant monolayer on compression (*10*). However, isotherm studies alone cannot reveal the molecular mechanisms by which SP-B alters fatty acid monolayers nor can they show if the peptide can produce similar morphological effects.

Direct images of the morphology and phase behavior of monolayers at the air-water interface obtained with epifluorescence microscopy can provide such information (*13*), but there are few such studies of lung surfactant monolayers (*14*, *15*) and, as far as we know, none that examines the effects of SP-B on the phase behavior of fatty acid monolayers. Our fluorescence images show that both SP-B and SP-B_{1-25} are incorporated into PA monolayers and form a new "fluid" phase that inhibits the formation of condensed phases at all surface pressures, π. This protein-induced fluid phase forms a network that breaks up the remaining condensed-phase domains at all π values up to collapse (*16*). As the size of the condensed-phase domains shrinks, the likelihood of heterogeneous nucleation of monolayer collapse is reduced by the protein-rich, fluid-phase network, leading to (i) lower ultimate γ values on compression and (ii) smaller and more homogeneous collapse structures that are easier to respread on expansion. The network is stabilized by the low line tension between the fluid phase and the condensed-phase domains, as evidenced by our observations of extended linear domains or "stripe" phases at low π values (*17*, *18*). Similar stripe phases were found in monolayers of fluorescein-labeled SP-B_{1-25}, suggesting that the protein lowers the two-dimensional (2D) line tension between phases and increases the ratio of fluid to condensed phases. The close correspondence between the isotherms and the morphology of lipid monolayers containing SP-B_{1-25} or SP-B confirms the results of a number of previous studies that show similar surface activity in model surfactant mixtures containing SP-B_{1-25} both in vitro and in vivo (*7*, *10*, *19*).

Monolayers of PA (Sigma, 99%) with various concentrations of either SP-B or SP-B_{1-25} were spread quantitatively from chloroform (Fisher Spectranalyzed) solution onto either a pure water (pH 5.5, Milli-Q, Millipore) or a $NaHCO_3$-buffered saline (pH 6.9, 150 mM NaCl, Sigma) subphase. Experiments were carried out at either 16°C, below the triple point of PA, or at 25° or 27°C, above the triple point (*20*). A custom-built microfluorescence film balance was used for all experiments (*21*, *22*).

The isotherm of PA at 16°C on a buffered saline subphase showed two distinct condensed phases: a compressible liquid-condensed phase (Fig. 1A, point a to point b), and a second, less compressible, solid-condensed phase (point b to point c), followed by collapse at ~43 mN/m (*13*). Adding SP-B_{1-25} caused the monolayer collapse pressures to increase significantly, in agreement with the observations of Longo *et al.* (*10*). As the fraction of SP-B_{1-25} was increased, the onset of the first pressure rise occurred at successively greater surface areas (see lift-off points in Fig. 1A), indicating that the water-soluble peptide was retained in the monolayer. Incorporation of SP-B in the monolayer showed the greatest increase in collapse pressure, to almost 70 mN/m, or at a γ near zero. Similar results were obtained on a pure water subphase at the same temperature, although with a less dramatic increase in collapse pressure (*23*). The additional increase in collapse pressure on buffered saline is likely due to the increased fatty acid dissociation at higher pH and ionic strength, which in turn increases

M. M. Lipp, K. Y. C. Lee, J. A. Zasadzinski, Department of Chemical Engineering, University of California, Santa Barbara, CA 93106, USA.
A. J. Waring, Martin Luther King Jr.–Drew University Medical Center and Perinatal Laboratories, Harbor–University of California, Los Angeles, CA 90059, USA.
*To whom correspondence should be addressed. E-mail: gorilla@engineering.ucsb.edu

the activation energy for monolayer collapse (*24*, *25*).

The PA isotherms at 25°C on buffered saline (Fig. 1B) were qualitatively similar to the low-temperature case except for the presence of a liquid-expanded region after lift-off, followed by a plateau where liquid-expanded and liquid-condensed phases coexist. Further increases in pressure led to the liquid-condensed phase and then the solid-condensed phase, and eventually to monolayer collapse at 52 mN/m (Fig. 1B). Addition of protein or peptide resulted in a rise in collapse pressures, and lift-off areas, similar to the situation with low-temperature films. The differences between SP-B and SP-B_{1-25} addition were much smaller at the more physiological, higher temperature (Fig. 1B).

Fluorescence micrographs of pure PA monolayers at 16°C on pure water (Fig. 2A) show that compressing the system past the lift-off area led to the formation of a uniform gray liquid–condensed phase. A new bright phase appeared that coexisted with the gray liquid–condensed phase when SP-B_{1-25} was added (Fig. 2A) (similar behavior was observed when SP-B was used). As the amount of peptide increased, the average size of the condensed-phase domains decreased while their number density increased. The peptide apparently disorders or "melts" the condensed phase of PA as the dye partitions into the new, peptide-rich "fluid" phase. Complexation of the positively charged protein or peptide with the negatively charged PA may be stabilized by electrostatics (*10*, *25*) and hydrophobic interactions.

In a corresponding system of PA at 25°C on buffered saline (Fig. 2, B to D), the darker liquid-condensed phase nucleates from the brighter liquid-expanded phase at the beginning of the coexistence plateau (see Fig. 1B, point d). In the absence of the peptide, dark liquid-condensed domains nucleated with low number density from the bright phase and grew into large domains (Fig. 2B). Increasing the fraction of SP-B_{1-25} or SP-B increased the number density of domains while the average domain size successively decreased (Fig. 2, C and D), similar to the behavior below the triple point (Fig. 2A). In addition to creating the new fluid phase, addition of either SP-B or the shorter SP-B_{1-25} acted to decrease the average size of the condensed-phase domains while increasing the amount of interface; this behavior implies that the effective line tension between the two phases is low (*1*).

On further compression, we observed a dramatic difference in the nucleation, growth, and morphology of monolayer collapse (and collapse pressure, see Fig. 1) as SP-B_{1-25} was added to PA at 16°C and 27°C on a pure water subphase. Without the peptide, large, dendritic "crystals" that grew with time appeared at collapse. With the peptide present, very small, bright collapse structures nucleated simultaneously over the entire monolayer at a significantly higher π and remained small, even upon further compression (Fig. 3, A and B). Similar collapse structures were observed for films consisting of PA and SP-B.

The subdivision of the dark condensed-phase domains by a skeletal network of a light gray fluid phase was observable in the micrograph of the collapsed film at 27°C (Fig. 3B). The network thinned as the surface pressure increased but persisted even after the film collapsed, suggesting that the peptide–fatty acid complex was retained in the film. Similar networks were observed for monolayers composed of PA and SP-B_{1-25} and PA and SP-B with 20% by weight peptide or protein at temperatures both above (Fig. 4, B and C) and below the triple point on buffered saline subphases up to and after collapse.

The existence of the mesh provides an explanation for the difference in collapse pressures and morphology. Monolayer collapse occurs by a process of nucleation and growth. With the breakup of the condensed phase into small domains, the probability diminishes that a collapse "nucleus" can be found in a given domain (*26*). As a result, each domain must nucleate collapse independently, resulting in more uniform, homogeneous nucleation at higher π values. Even after this homogeneous nucleation, the growth of the collapse structures is lim-

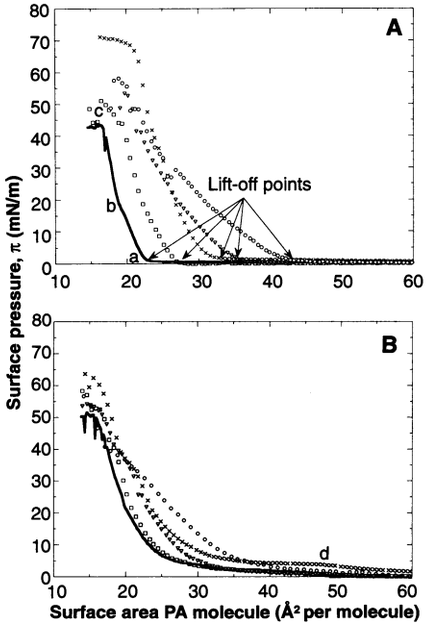

Fig. 1. Surface pressure, π, versus area per fatty acid molecule isotherms for mixtures of PA and SP-B_{1-25} and PA and SP-B (**A**) at 16°C and (**B**) at 25°C on a $NaHCO_3$-buffered saline subphase (pH 6.9, 150 mM NaCl). Symbols used are as follows: 0% by weight SP-B_{1-25} (solid trace); 5% by weight SP-B_{1-25} (squares); 10% by weight SP-B_{1-25} (inverted triangles); 20% by weight SP-B_{1-25} (circles); and 20% by weight SP-B (crosses). The point marked a signifies the beginning of the liquid-condensed phase; b signifies the transition to the solid-condensed phase; c signifies the film collapse; and d [in (B)] signifies the beginning of the liquid-expanded–liquid-condensed coexistence. The peptide increases the collapse pressure of the monolayer, leading to lower γ values on compression. All mixtures contain less than 1 mol % (with respect to the PA concentration) NBD-HDA, which does not alter the isotherms significantly.

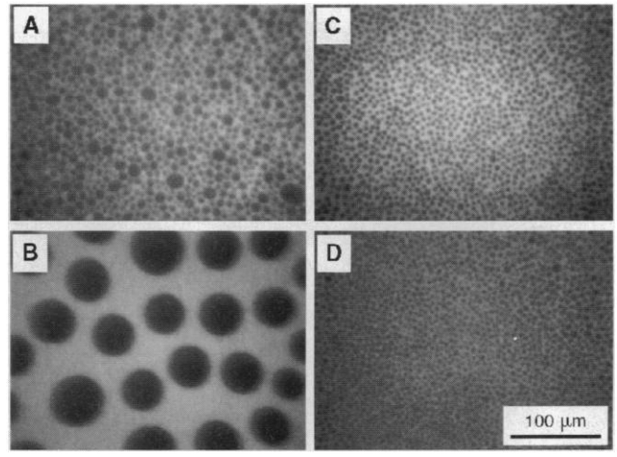

Fig. 2. Fluorescence micrographs of mixtures of PA and SP-B_{1-25} and PA and SP-B: (**A**) 20% by weight SP-B_{1-25} at 16°C on a pure water subphase; (**B**) 0% by weight SP-B_{1-25}; (**C**) 20% by weight SP-B_{1-25}; and (**D**) 20% by weight SP-B at 25°C on a buffered saline subphase. All mixtures contain less than 1 mol % (with respect to the PA concentration) NBD-HDA. Image (A) was taken at the lift-off point, and images (B) to (D) at an area per PA molecule of 35 Å² (in the liquid-expanded–liquid-condensed coexistence region). The peptide inhibits the formation of the condensed phase, leading to the formation of a disordered, bright fluid phase that separates the remaining condensed-phase domains. The line tension between the two phases is small, as indicated by a steady decrease in the size of the condensed-phase domain with increasing peptide concentration. The image contrast results from the exclusion of the dye from the more ordered, condensed phases (dark) and its incorporation in the more disordered, expanded phases (bright).

ited by the finite size of the condensed domains; hence, the respreading of these small collapse structures on expansion occurs much more readily. The formation of a fluid-phase network in the presence of SP-B that breaks up the condensed-phase domains alters the nucleation and growth of monolayer collapse, leading to lower ultimate γ values on compression and easier respreading on expansion.

The network formation that breaks up the condensed domains requires a large amount of interface and hence a low line tension between the fluid and condensed phases. These low line tensions also appear to form in the presence of SP-B, as evidenced by the formation of "stripe" phases at low π values (Fig. 4). When a mixture of PA with a high percentage of SP-B_{1-25} (20 or 30% by weight) was spread on buffered saline at 16°C, alternating linear domains of high and low lipid concentration, or stripe phases (*17*), were observed at zero applied pressure (Fig. 4A). In mixed lipid and protein monolayers, we also observed that circular domains undergo shape transitions to form labyrinthine patterns (*27*) upon compression at zero π (Fig. 4D).

Several researchers have observed stripe phases and shape transitions in monolayers at the air-water interface (*28*). The transition between circular and stripe domains (Fig. 4D) can be understood in terms of a competition between the line tension at the domain boundary and the electrostatic repulsion within the domain. In the limit of large line tensions, circular domains minimize the length of the domain boundary. As the line tension decreases relative to the repulsive interactions within the domains, elongated shapes or stripe phases form. In view of the fact that stripes were not observed in mixed monolayers with low protein content even on a buffered saline subphase but were present in pure fluorescein-tagged protein (*29*) monolayers on a pure water subphase, we believe that the stripe patterns are inherent to the protein. These results, combined with theoretical and experimental observations that stripe formation typically occurs in mixed monolayers (*18, 30*) suggest that the protein undergoes some combination of conformational, orientational or aggregational change induced by π. Protein conformational changes induced by both π and the lipid environment have been observed to occur in similar systems (*31*).

The full-length SP-B and the SP-B_{1-25} peptide are incorporated into PA monolayers and inhibit the formation of solid-condensed phases at all π values. The resulting protein-rich fluid phase forms a network separating the condensed phase domains at π values up to collapse. In pure PA monolayers, collapse occurs by the nucleation and growth of large, 3D dendritic "crystals" from the solid-condensed phase. With the presence of the peptide or the protein a new type of nucleation occurs at higher π values (lower γ values), thereby removing any driving force for the squeeze-out of either the protein or the fatty acid. These new collapse structures occur much more uniformly across the monolayer, are much smaller in size, and hence, are much easier to respread on lowering the surface pressure. Stripe patterns, indicative of low line tensions, are found both in fatty acid films with high percentage of protein on buffered saline subphase and in films formed by fluorescein-tagged SP-B_{1-25} on pure water subphase, and these patterns help explain the stability of the fluid phase network. This detailed picture of the role of SP-B and SP-B_{1-25} in the monolayer should make it possible to develop synthetic peptides or even simple polymers that can be used as replacement surfactants. These results

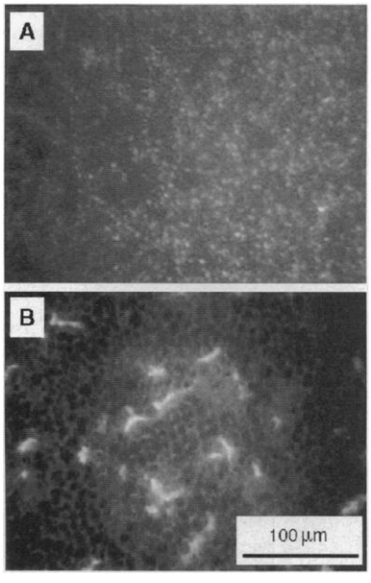

Fig. 3. Collapse structures of PA films with SP-B_{1-25} on a water subphase at two different temperatures. (**A**) Small, bright collapse structures nucleate from condensed-phase domains on the collapse of monolayers of a mixture of PA and 20% by weight SP-B_{1-25} at 16°C. The small spots disappear quickly on respreading. (**B**) A network of bright "fluid" phases remains at collapse pressure for a mixture of PA and 20% by weight SP-B_{1-25} at 27°C. Small, bright collapse structures nucleate uniformly across the monolayer, and respreading is easy.

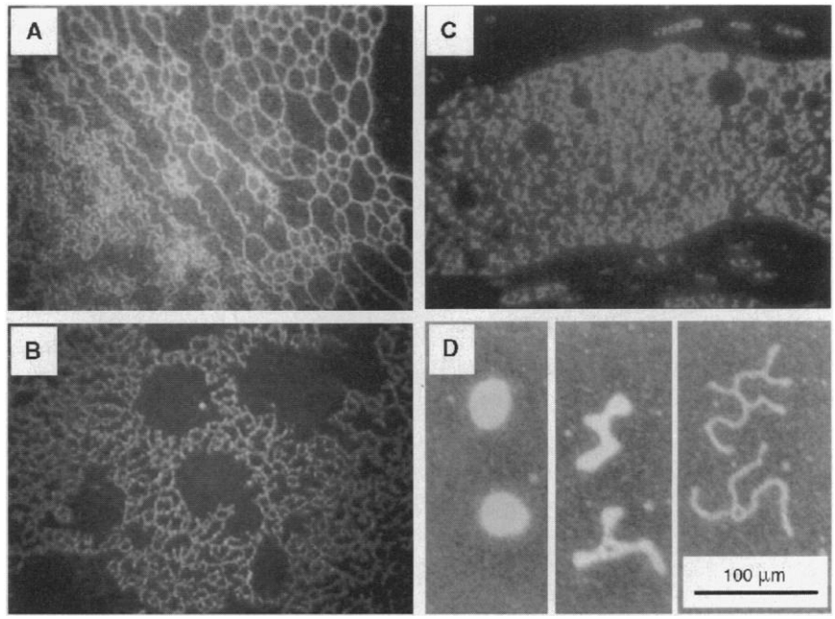

Fig. 4. (**A**) Fluorescence micrographs of stripe patterns observed in a monolayer from a mixture of PA and SP-B_{1-25} (20% by weight peptide) on a buffered saline subphase at 16°C and zero surface pressure. (**B** and **C**) A network of bright "fluid" phases observed near the collapse pressure for (B) a mixture of PA and 20% by weight SP-B_{1-25}, and (C) a mixture of PA and 20% by weight SP-B at 16°C on a buffered saline subphase, separating regions of dark condensed phase. (**D**) A sequence in which two bright circular domains in a mixture of PA and 20% by weight SP-B_{1-25} on a buffered saline subphase transform into two labyrinthine patterns with decreasing surface area at zero surface pressure. The transformation shows that the ratio of electrostatic repulsion within the domain to the line tension at the domain boundary is changing on compression, perhaps as a result of a conformational change in the protein.

show that many of the essential features of the whole protein are captured by the NH_2-terminal segment.

REFERENCES AND NOTES

1. Surface tension, γ, is the force per unit area exerted on the 2D interface between two coexisting phases in three dimensions. Similarly, line tension is the force per unit length exerted on the 1D interface between two coexisting phases in two dimensions. Surface pressure, π, is the difference between the γ of pure water (72 mN/m) and the measured γ with the monolayer present. The collapse pressure of a monolayer is the highest π or lowest γ attainable before the film collapses or ejects material into a bulk phase.
2. D. L. Shapiro and R. H. Notter, Eds., *Surfactant Replacement Therapy* (Liss, New York, 1989).
3. M. E. Avery and J. Mead, *Am. J. Dis. Child.* **97**, 917 (1959); W. Seeger *et al.*, *Am. J. Physiol.* **261**, L286 (1992).
4. R. Soll, *Resident Staff Physician* **38**, 19 (1992).
5. J. A. Whitsett *et al.*, *Pediatr. Res.* **20**, 460 (1986); S. Hagwood *et al.*, *Proc. Natl. Acad. Sci. U.S.A.* **84**, 66 (1987); S.-H. Yu and F. Possmayer, *Biochem. J.* **236**, 85 (1986).
6. Two larger lung surfactant–specific proteins, SP-A and SP-D, are also present in lung surfactant but do not contribute to surface activity.
7. M. Longo, A. Waring, J. A. Zasadzinski, *Biophys. J.* **63**, 760 (1992).
8. A. Cockshutt, D. Absolom, F. Possmayer, *Biochim. Biophys. Acta* **1085**, 248 (1991); J. B. Chung *et al.*, *Langmuir* **6**, 1647 (1990); N. Mathialagan and F. Possmayer, *Biochim. Biophys. Acta* **1045**, 121 (1990); S.-H. Yu and F. Possmayer, *ibid.* **1126**, 26 (1992).
9. SP-B and SP-B_{1-25} were synthesized and analyzed as described in (*10*), except that, for the human 78-residue protein SP-B, we used an ABI 431A peptide synthesizer (Applied Biosystem, Foster City, CA) applying FastMoc chemistry (*11*). Amino acid residues 26 to 59 of SP-B were double-coupled; all other residues were single-coupled. After cleavage from the resin, we purified the peptide by reverse-phase high-performance liquid chromatography (HPLC) with a Vydac C4 column (Vydac, Hesperia, CA), using a water-acetonitrile gradient containing 0.1% trifluoroacetic acid. The formation of disulfide bonds was facilitated with the use of EKATHIOX resin (Ekagen, Palo Alto, CA). Oxidation with EKATHIOX resin was carried out by addition of a 1 mM peptide solution of trifluoroethanol:water (8:2 v/v) to a 10-fold molar excess of the resin-active group to peptide thiol. The reaction was allowed to proceed for 6 hours before the peptide in solution was separated from the resin by centrifugation (1000*g*, 10 min). The monomeric oxidized state was confirmed by matrix-assisted laser desorption–time of flight (MALDI-TOF) mass spectroscopy. The conformation of SP-B in the PA multilayer was largely helical as determined by Fourier-transform infrared spectroscopy measurements.
10. M. L. Longo, A. M. Bisagno, J. A. N. Zasadzinski, R. Bruni, A. J. Waring, *Science* **261**, 453 (1993).
11. C. G. Fields *et al.*, *Pept. Res.* **4**, 95 (1991).
12. M. L. Longo, thesis, University of California, Santa Barbara (1993).
13. H. Möhwald, *Annu. Rev. Phys. Chem.* **41**, 441 (1990); H. M. McConnell, *ibid.* **42**, 171 (1991); C. M. Knobler and R. C. Desai, *ibid.* **43**, 207 (1992).
14. J. Perez-Gil *et al.*, *Biophys. J.* **63**, 197 (1992).
15. A. Post *et al.*, *Mol. Membr. Biol.* **12**, 93 (1995).
16. A similar fluidizing effect was observed in monolayers of DPPC with SP-B and SP-C by K. M. Keough and co-workers [K. Nag *et al.*, *Biophys. J.* **71**, 246 (1996)].
17. M. Seul and D. Andelman, *Science* **267**, 476 (1995).
18. H. M. McConnell and V. T. Moy, *J. Phys. Chem.* **92**, 4520 (1988).
19. V. Sarin *et al.*, *Proc. Natl. Acad. Sci. U.S.A.* **87**, 2633 (1990).
20. The triple point denotes the location in the phase diagram where the 2D equivalents of the solid (liquid-condensed), liquid (liquid-expanded), and gaseous phases coexist at equilibrium. The triple-point temperature of PA on a Milli-Q water subphase is 24.8°C; the triple-point temperature of PA on a buffered saline subphase is lower. Below the triple point, the gaseous phase transforms into the liquid-condensed phase without going through the liquid-expanded phase. Above the triple point, the liquid-condensed and liquid-expanded phases coexist.
21. Details of the experimental setup will be published elsewhere (K. Y. C. Lee *et al.*, in preparation). All mixtures contained less than 1 mol % of *N*-7-nitrobenz-2-oxa-1,3-diazol-4-yl-hexadecylamine (NBD-HDA, Molecular Probes) to provide for image contrast (*22*). Monolayers were spread at a highly expanded state; the monolayer area was compressed at various speeds ranging from 0.01 to 0.05 Å^2 per molecule per second, while the surface pressure, area, and the morphology of the film were continuously monitored. The compression speed was held constant within each set of measurements for quantitative comparisons.
22. The fluorescent dye molecules preferentially partition into the less ordered phase (the more condensed or better ordered phase has tighter packing and excludes the dye). This behavior results in the assignment of the brighter liquid-expanded phase and the darker liquid-condensed phase observed in fluorescence microscopy. NBD-HDA quenches when it is in contact with the subphase, rendering the gaseous phase black.
23. On a pure water subphase at 16°C, collapse pressures and lift-off areas increased as the fraction of SP-B_{1-25} was increased. Collapse pressures were lower than those observed on a buffered saline subphase; the highest collapse pressure achieved was ~54 mN/m. A similar weight fraction of the SP-B produced a similar rise in the collapse pressure. The full-length protein, which is less water-soluble, appears to be better retained in the monolayer than the shorter peptide.
24. R. Smith and J. Berg, *J. Colloid Interface Sci.* **74**, 273 (1980); S. Xu *et al.*, *ibid.* **89**, 581 (1982).
25. J. Perez-Gil, C. Casals, D. Marsh, *Biochemistry* **34**, 3964 (1995).
26. A. W. Adamson, *Physical Chemistry of Surfaces* (Wiley, New York, ed. 5, 1990); R. J. Hunter, *Foundations of Colloid Science* (University Press, Belfast, 1992), vol. 1, chap. 5. The nucleation sites for heterogeneous nucleation in three dimensions are typically dust or other materials that provide a good surface for the condensation of the solid phase. In 2D films, the identity of the nuclei is less clear.
27. K. Y. C. Lee and H. M. McConnell, *J. Phys. Chem.* **97**, 9532 (1993); A. J. Dickstein, S. Erramilli, R. E. Goldstein, D. P. Jackson, S. A. Langer, *Science* **261**, 1012 (1993).
28. H. M. McConnell, *Nature* **310**, 47 (1984); M. Seul and M. J. Sammon, *Phys. Rev. Lett.* **64**, 1903 (1990); M. Seul and V. S. Chen, *ibid.* **70**, 1658 (1993).
29. We synthesized the fluorescein derivative of SP-B_{1-25} with linkages at cysteine residues 8 and 11 by slowly adding a fivefold excess of fluorescein-5-maleamide (Molecular Probe) in dimethylformamide to the peptide in 100 mM to 10 mM phosphate buffer (pH 6.5). The mixture was bath-sonicated for 5 min and vortexed immediately for 1 hour at 25°C. The reaction was then quenched with a twofold excess of cysteine, and the reaction mixture was dialyzed against distilled water overnight. The peptide was then freeze-dried and purified by reversed-phase HPLC.
30. J. Stine and D. T. Stratmann, *Langmuir* **8**, 2509 (1992).
31. M. Briggs *et al.*, *Science* **233**, 206 (1986); J. Seelig *et al.*, *Mol. Membr. Biol.* **12**, 51 (1995); L. M. Gordon *et al.*, *Protein Sci.* **5**, 1662 (1996).

32. We thank D. K. Schwartz, C. Knobler, R. Stuber, and A. Weinberg for help with trough construction; K. Faull and R. Stevens for help with the mass spectral analysis; and L. Gordon for his reading of the manuscript. The work of J.A.Z., M.M.L., and K.Y.C.L. was supported by NIH grant HL51177-02; K.Y.C.L. received a University of California President's postdoctoral fellowship; and M.M.L. received a University of California Regents graduate fellowship. The work of A.J.W. was supported by NIH grant HL55534 and NIH Small Equipment grant GM 50483.

6 February 1996; accepted 16 July 1996

Attomole Protein Characterization by Capillary Electrophoresis–Mass Spectrometry

Gary A. Valaskovic, Neil L. Kelleher, Fred W. McLafferty*

Electrospray ionization with an ultralow flow rate (≤4 nanoliters per minute) was used to directly couple capillary electrophoresis with tandem mass spectrometry for the analysis and identification of biomolecules in mixtures. A Fourier transform mass spectrometer provided full spectra (>30 kilodaltons) at a resolving power of ≈60,000 for injections of 0.7×10^{-18} to 3×10^{-18} mole of 8- to 29-kilodalton proteins with errors of <1 dalton in molecular mass. Using a crude isolate from human blood, a value of 28,780.6 daltons (calculated, 28,780.4 daltons) was measured for carbonic anhydrase, representing 1 percent by weight of the protein in a single red blood cell. Dissociation of molecular ions from 9×10^{-18} mole of carbonic anhydrase gave nine sequence-specific fragment ions, more data than required for unique retrieval of this enzyme from the protein database.

The molecular elucidation of biochemical events at the cellular and subcellular level is increasingly dependent on innovative methodologies for molecular characterization and imaging (*1*). These techniques have been especially successful for preselected specific ("targeted") compounds, but their ability to reveal and characterize unknown biomolecules at the single-cell level is limited. Molecular complexity is a primary problem. Microcolumn mixture separation, especially capillary electrophoresis (CE) (*2*), can efficiently and rapidly separate $<10^{-10}$-liter samples to detect attomole (10^{-18} mol) components, a level suitable for minor component analysis in a

Department of Chemistry, Baker Laboratory, Cornell University, Ithaca, NY 14853, USA.

*To whom correspondence should be addressed.